Lab #6

Stepper Motor

MECHENG 552

Team 4B

Saptadeep Debnath
Manavendra Desai
Ellen Kim
David Radtke

Professor Shorya Awtar
10 December 2019

Department of Mechanical Engineering
University of Michigan, Ann Arbor

Contents

List of Figures

List of Tables

1 Stepper Motor Driver (33pts)

(a) Electrical Wiring Diagram (10)

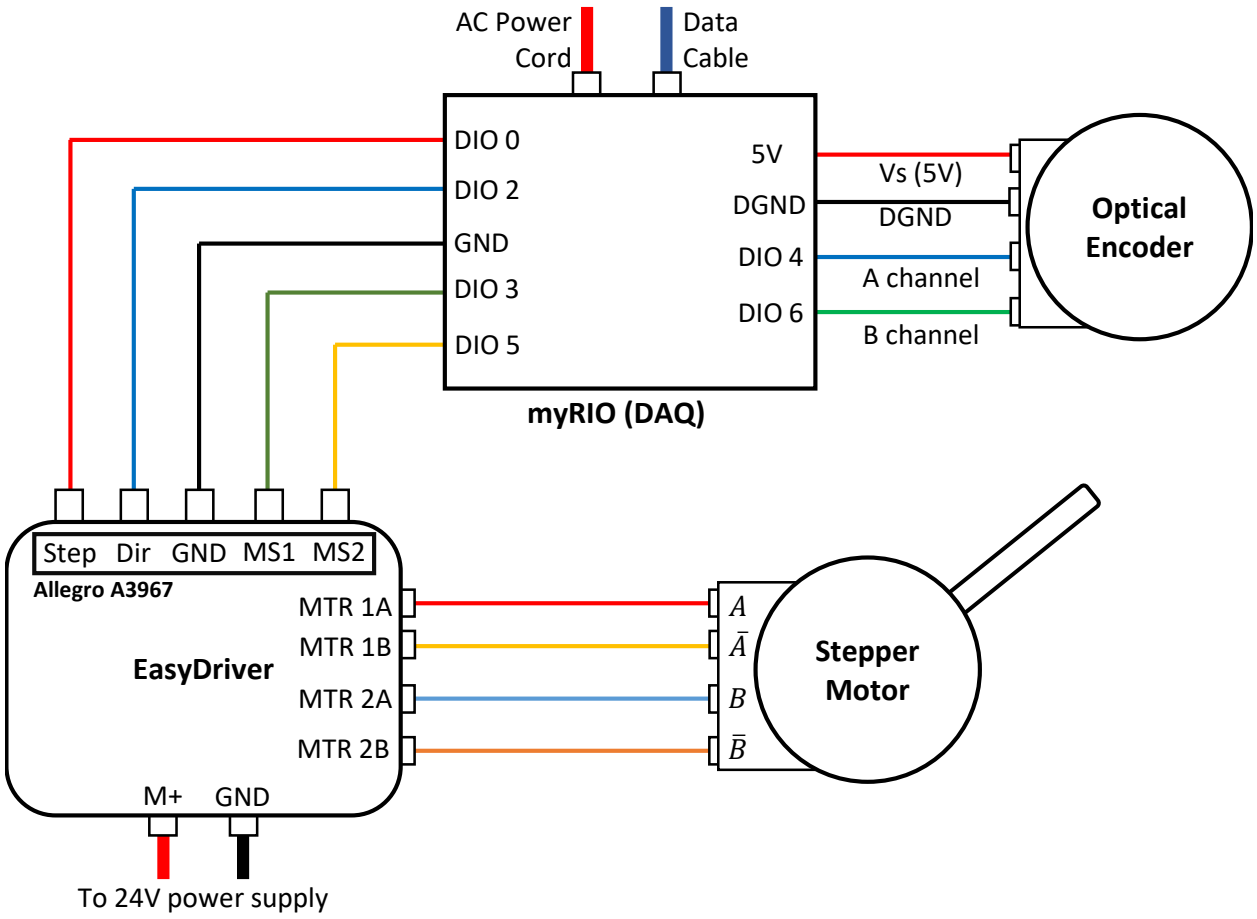

Figure 1: Electrical Wiring Diagram for the current stepper motor setup.

The complete wiring diagram shown in figure 1 comprises of four major components; stepper motor, EasyDriver with A3967SLB microstepping motor driver, an optical encoder and the data acquisition unit (myRIO), which in conjunction are used to drive the motor, detect its angular position and compute its angular velocity. Pulse train (Step) is generated corresponding to either a commanded angular position or an angular velocity by the LabVIEW VI which is then parsed to the EasyDriver via myRIO along with the direction (Dir) and the step logic, i.e. full step, half step, quarter step or micro step ($1/8^{th}$ step) using MS1 and MS2 pin on EasyDriver. These commands are then translated to corresponding current input to the motor. The input voltage for the motor is provided by the EasyDriver via an external power supply of 24V, whereas the control logic is operated on 5V from the analog output of myRIO. The optical encoder used to measure the angular position of the stepper motor is powered via the myRIO's 5V power output.

(b) A3967 Chip Functionality (10)

Table 1: Pin functionality and required connections for A3967. Pins like RESET, ENABLE, and SLEEP that have a bar over them in the datasheet are active-low pins which means that they need 5V to turn off.

#	Pin	Functionality	What Should it be connected to
1	REF	The voltage into this pin determines the max current output from the driver.	The easy driver allows for an adjustable max current via a potentiometer intermediate to the 5V logic supply.
2	RC2	The resistance and capacitance connected to this pin define the off-time of H-bridge 2, which is the portion of the duty-cycle where no current is supplied.	It is connected to a resistor and capacitor internal to the EasyDriver.
3	$\overline{SLEEP}$	Active-low pin which disables the driver. HIGH allows operation of driver.	It is connected to the Vcc supplied by the myRio, via a path supplied by the EasyDriver.
4	OUT2B	H bridge 2 output B. It is one of the power connections to coil B of the stepper motor.	This pin must be connected to coil B of the motor, which is made external to the easy driver.
5	LOAD SUPPLY2	Power supply for bridge 2	Connected to the 24V power supply, external to the easy driver
6	GND	Ground	All grounds of the chip are connected to each other within the easy driver, which is given a common ground via a pin to the external circuit.
7	GND	Ground	See 6
8	SENSE2	Sense resistor for bridge 2. The max current to the motor from bridge 2 is a function of the resistance connected from this pin to ground.	This pin is connected to the EasyDriver ground with an intermediate resistor.
9	OUT2A	H bridge 2 output A. It is one of the power connections to coil B of the stepper motor.	Connected to coil B of the motor, an external connection
10	STEP	Low-to-high transition of voltage input to this pin advances the motor one increment as defined by the states of MS1 and MS2	Connected to a digital output pin of the myRio
11	DIR	State of this pin determines direction of rotation.	Connected to a digital output pin of the myRio
12	MS1	Via a HIGH or LOW input voltage to this pin and MS2, any of four motor increment sizes can be chosen	Connected to a digital output pin of the myRio
13	MS2	Via a HIGH or LOW input voltage to this pin and MS1, any of four motor increment sizes can be chosen	Connected to a digital output pin of the myRio
14	LOGIC SUPPLY	5V or 3.3 V supply used for logic purposes	Connected to a digital output pin of the myRio
15	$\overline{ENABLE}$	Active-low input that enables all outputs. Unlike RESET, this pin does not affect inputs	Connected to a LOW input/GND, which is provided within EasyDriver
16	OUT1A	H bridge 1 output A. Is one of the power connections to coil A of the stepper motor.	Connected to coil A of the motor, an external connection
17	SENSE1	Sense resistor for bridge 1. The max current to the motor from bridge 1 is a function of the resistance connected from this pin to ground.	Connected to the EasyDriver
18	GND	Ground	See 6
19	GND	Ground	See 6
20	LOAD SUPPLY 1	Power supply for H bridge 1	Connected to the 24V power supply, external to the easy driver
21	OUT1B	H bridge 1 output B. Is one of the power connections to coil A of the stepper motor.	Connected to coil A of the motor, an external connection
22	$\overline{RESET}$	Active low turns off outputs and ignores STEP inputs until set to HIGH	Connected to a HIGH voltage input which is ultimately provided by the myRio
23	RC1	The resistance and capacitance connected to this pin define the off-time of H-bridge 1, which is the portion of the duty-cycle where no current is supplied.	Connected to a resistor and capacitor internal to the EasyDriver
24	PFD	Mixed-decay setting. The driver can either wind down the motor current using its own back-emf(slow decay) or by actively applying a voltage in the opposite direction(fast decay). Mixed Decay is the application of one method or the other depending on where the motor is in its decay cycle. The voltage applied to this pin decides where the switchover from slow to fast decay is.	

(c) EasyDriver PCB (10)

Sleep - The sleep pin is hardwired to a HIGH state because in the low state the driver would be asleep and not perform any operations to minimize power consumption. We did not have to change this value because whenever the driver and stepper motor were not in use, the power supply was turned off. As a result, we never used this pin and avoided additional wiring.

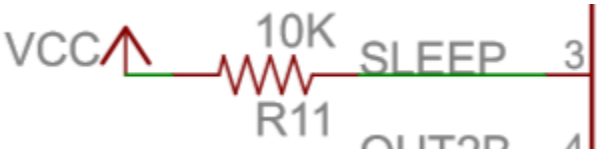

Figure 2: Wiring diagram for SLEEP.

Enable - Enable is hardwired to ground which achieves its active LOW state which allows the driver to output current commands to the motor. We did not change this because while using the driver we always wanted to output commands to the motor if a step input was given. In fact, we never used this pin and avoided additional wiring.

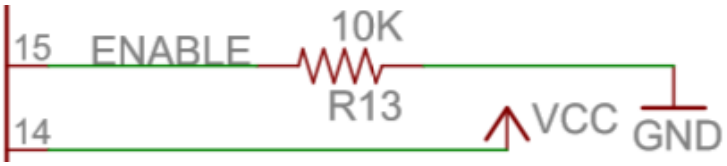

Figure 3: Wiring diagram for ENABLE.

MS1 - MS1 is defaulted to the high state, which corresponds to half and eighth steps. This pin is also connected to a digital output from the myRio as well as being connected to VCC. This pin's voltage is changed to low whenever full or quarter steps are desired. When a voltage of zero is delivered from the myRio, the pin's voltage goes to zero and likewise when the myRio signal goes to HIGH, the pin's voltage goes to HIGH. Since both MS1 and MS2 are defaulted to HIGH, it seems it was the creators intent to use eighth stepping as the default movement style. Perhaps for its high resolution.

Figure 4: Wiring diagram for MS1.

MS2 - MS2 is defaulted to the high state, which corresponds to quarter and eighth steps. This pin is also connected to a digital output from the myRio as well as being connected

to VCC. This pin's voltage is changed to low whenever full or half steps are desired. When a voltage of zero is delivered from the myRio, the pin's voltage goes to zero and likewise when the myRio signal goes to HIGH, the pin's voltage goes to HIGH. Since both MS1 and MS2 are defaulted to HIGH, it seems it was the creators intent to use eighth stepping as the default movement style. Perhaps for its high resolution.

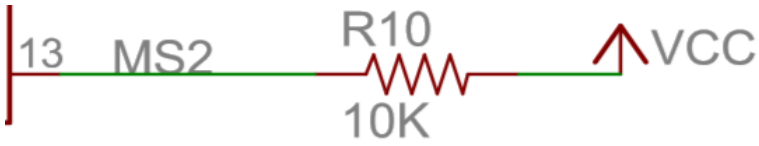

Figure 5: Wiring diagram for MS2.

(d) Power for Optical Encoder (3)

We supplied the 5V for the optical encoder from a digital output from the myRio instead of using an external power supply or from the EasyDriver PCB. The EasyDriver PCB's advantage is that the current does not fluctuate with load; however, because the power supply from the EasyDriver needs to pass through the PCB, it adds noise into the power signal. The power supply on the other hand has a clean power signal; however, its current fluctuates with load.

2 LabVIEW Program (20pts)

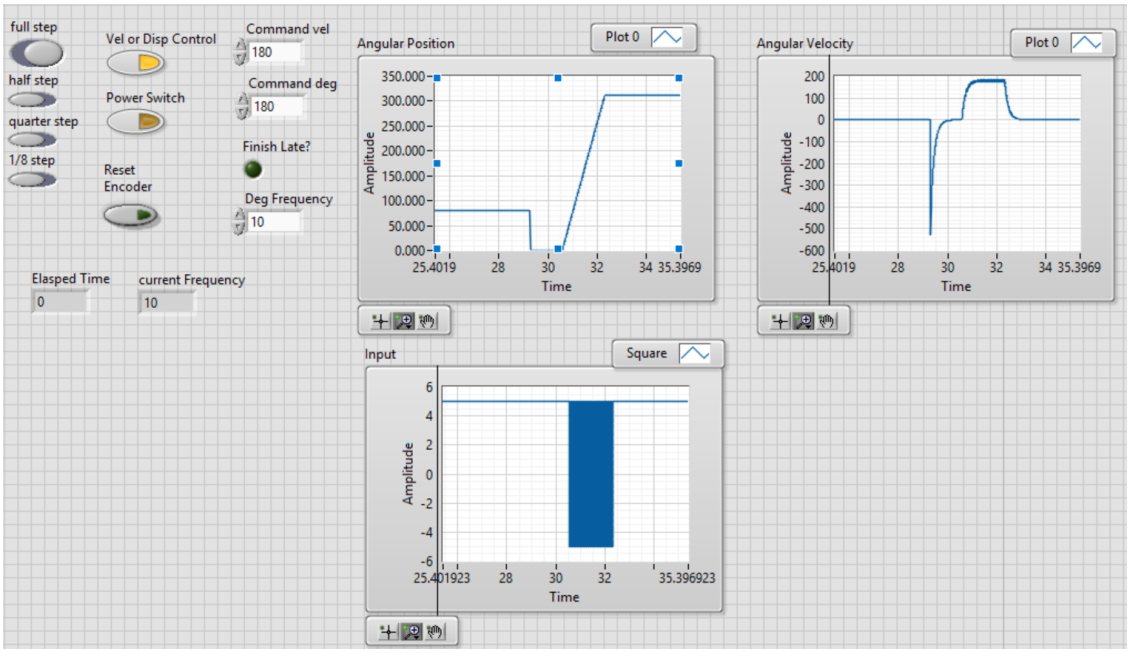

Figure 6: Front panel of the VI for position and velocity control.

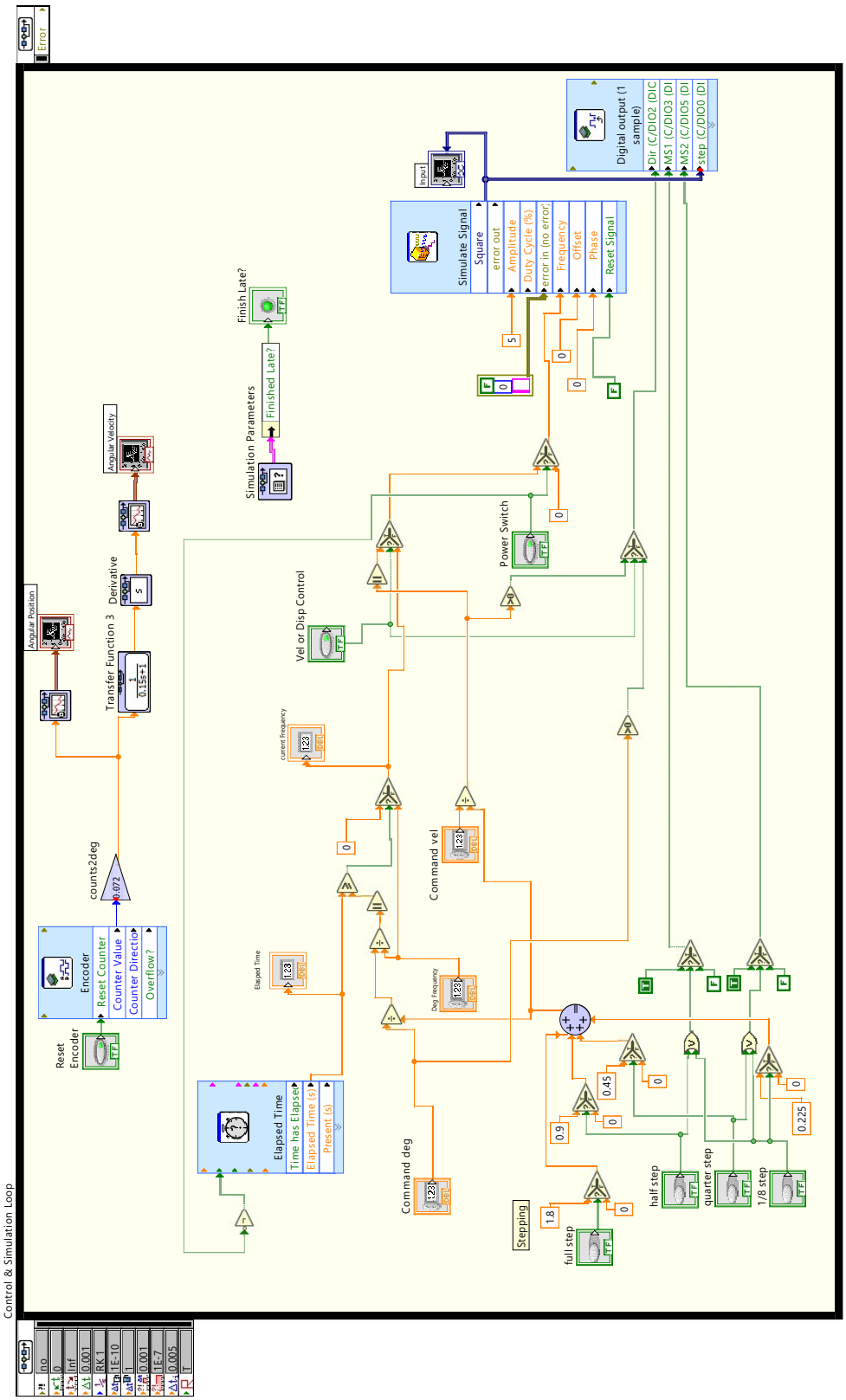

Figure 7: Block diagram of the VI for position and velocity control.

3 Experimental Characterization (88pts)

(a) One Full Step of Motor (66)

Rise Time, Over-shoot, Oscillations, Steady-state error: The stepper motor was commanded to move by one full step. The observation and discussion related to the displacement response of the rotor using encoder measurement is shown below. Each of the observed behavior was fitted with a smoothing spline curve in MATLAB because the optical encoder is limited in resolution.

With Load (10): When the stepper motor was attached to the motion system with belt and output shaft, its response to a step command is shown in figure 8 with its properties shown in table 2.

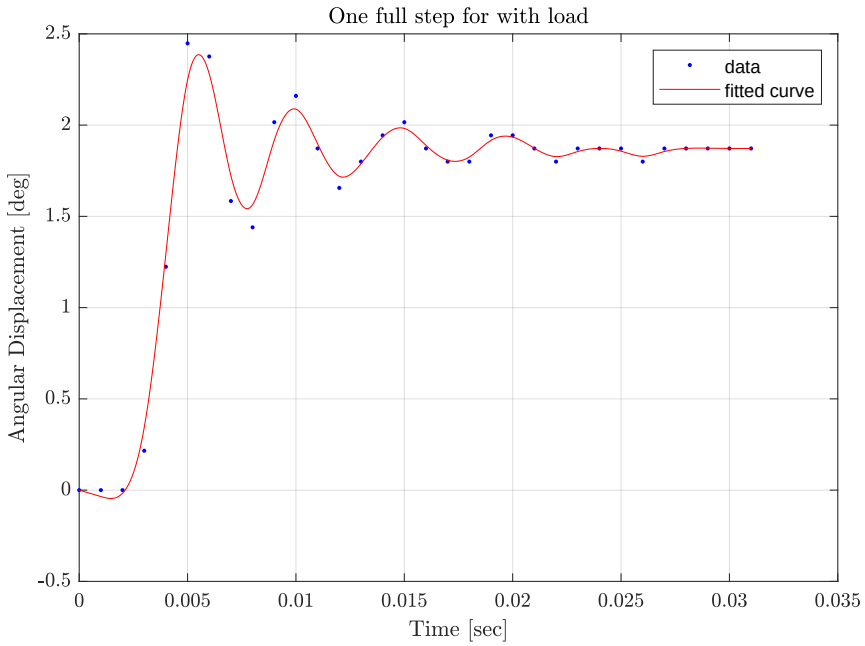

Figure 8: Step response of motor with load. When the motor takes 1.8 degree step, it shows oscillations in its behavior captured in the plot above.

Table 2: Properties of step response of motor with load.

Properties	Values
Rise time	0.003 sec
Over-shoot	30.77%
Number of oscillations until decay	5
Steady-state error	3.85%

Without Load (10): Similarly, when the stepper motor was stand-alone, its response to a step command is shown in figure 8 with its properties shown in table 2. Compared to the

values with load, the without load property values indicate higher over-shoot and smaller steady-state error.

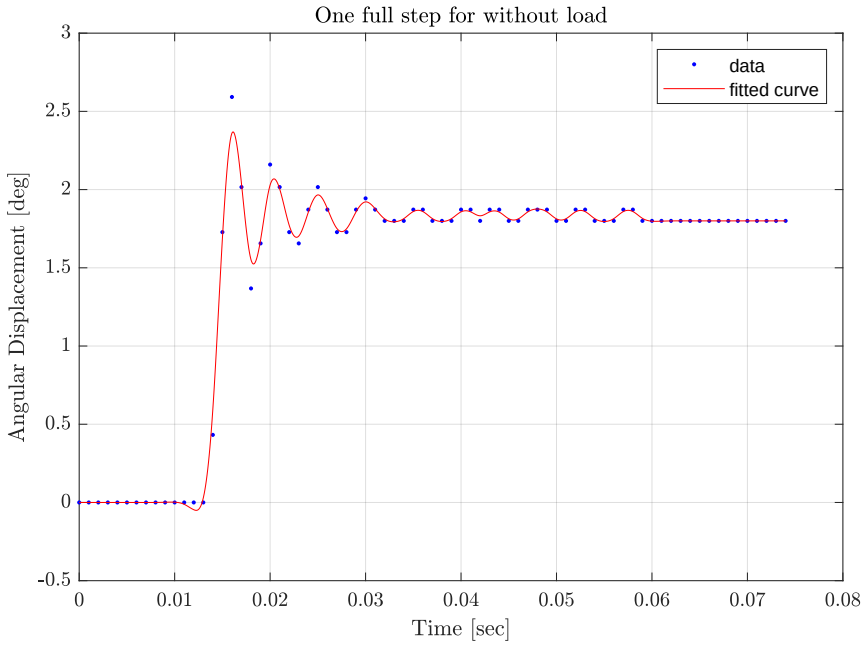

Figure 9: Step response of motor without load. When the motor takes 1.8 degree step, it shows oscillations in its behavior captured in the plot above.

Table 3: Properties of step response of motor without load.

Properties	Values
Rise time	0.003 sec
Over-shoot	44%
Number of oscillations until decay	10
Steady-state error	0%

Natural Frequency and Damping: Based on the measurements of the step response, the natural frequency and damping ratio associated with the stepper motor can be calculated. Looking at figure 8 and 9, the step response produces oscillations about 1.8 degrees. The system can thus be assumed as a second-order system and its transfer function, relating the commanded position input to the actual position output, is assumed to have the following form with two poles and no zeros:

$$G(s) = \frac{k_{dc}\omega_n^2}{s^2 + 2\xi\omega_n s + \omega_n^2}, \tag{1}$$

where k_{dc} is the DC gain, ω_n is the natural frequency, and ξ is the damping ratio. The DC gain is defined as the ratio of magnitude of the steady-state step response to the magnitude

of the step input. The natural frequency is found by

$$\omega_n = \frac{1}{t_n - t_{n+1}},$$

where it takes the inverse of the period of one cycle with t representing time. The damping ratio is defined as

$$\xi = \frac{1}{\sqrt{1 + (\frac{2\pi}{\delta})^2}}$$

where $\delta = \ln \frac{x_1}{x_2}$ and x is the amplitude at two successive peaks of the decaying oscillation.

With Load (10): The natural frequency of the motor with load is shown in table 4. Thus, using the transfer function in equation 1 and the values in table 4, the transfer function of stepper motor with load is defined as

$$G(s) = \frac{4.33E4}{s^2 + 41.63s + 4.16E4}.$$

Without Load (10): Similarly, using the transfer function in equation 1 and the values in table 4, the transfer function of stepper motor without load is defined as

$$G(s) = \frac{4.56E4}{s^2 + 33.11s + 4.74E4}.$$

Table 4: Natural Frequency and damping of step response of motor with and without load.

Properties	With Load	Without Load
DC Gain	1.04	1
Natural Frequency [Hz]	204.08	217.86
Damping Ratio	0.102	0.076

Dynamics: The (damped) natural frequency for the stepper motor system depends on inertia, stiffness and damping elements. Damping will be electromagnetic in nature when accounting for the back emf induced by the permanent magnet across the stator windings in a moving stepper motor rotor. Damping will be mechanical in nature when accounting for the viscous effects of the lubricant applied in-between the rotor shaft and its bearings. When the belt is on, there will be additional dry friction if the belt slips over the stepper motor rotor shaft and the load (pointer) shaft. Stiffness will be mechanical in nature if the belt is too stretched and adds lateral motion to the stepper motor rotor shaft. Stiffness will have an electromagnetic form too due to the torque-position characteristics of the stepper motor.

With Load (3): Every moving element in the stepper motor will contribute to its mechanical inertia. With the belt on, at the system level this mechanical inertia would have increased due to additional rotating elements in the form of the belt and pointer assembly. Inertia will

also have an electrical element in inductance of the stator windings, which manifests itself in the electrical time constant for the stepper motor.

Without Load (3): There is reduced inertia, magnetic stiffness, viscous and frictional damping than the stepper motor with load. However, there are still forms of damping without the dry friction from the belt.

Resonance and Lack of Synchronization The stepper motor was commanded to run at a constant velocity with the steps/sec equaling the natural frequencies in the two setup (i.e. with load and without load) found in the previous section. In addition to that, motor characteristics are recorded for a commanded steps/sec of integral multiples and integral fractions of the natural frequency. It is found that a buzzing noise that occurs when the motor runs on natural frequency, also happens when it is run at the integral multiples of the natural frequency. But even though we observe a similar response at the integral fractions of natural frequency, no noticeable buzzing sound can be heard. A maximum frequency is also recorded for when the motor stalls and loses synchronization.

With Load (10): As mentioned in the previous section the natural frequency of the system with the load attached to it is found to be around 204Hz. The natural frequency is estimated by extrapolating and fitting the curve using a Smoothing Spline method in MATLAB. Whereas while performing the experiment it is found that the system has a natural frequency of 200Hz as shown in figure 10(a), where the system is excited at 150Hz, 200Hz and 250Hz. Hence the error in the natural frequency of the system is calculated to be 2%. Next, the motor is excited at step-rates that are integral multiples and integral fractions of the natural frequency. As expected a similar response is observed at the integral fraction (100Hz) and the integral multiple (400Hz) of the natural frequency. Response at these three frequencies (100Hz, 200Hz and 400Hz) exhibit a higher band of velocity than at any other frequency (300Hz), as seen in figure 11. The system however shows unstable performance (lack of synchronization) at 1.6KHz as shown in figure 10(b).

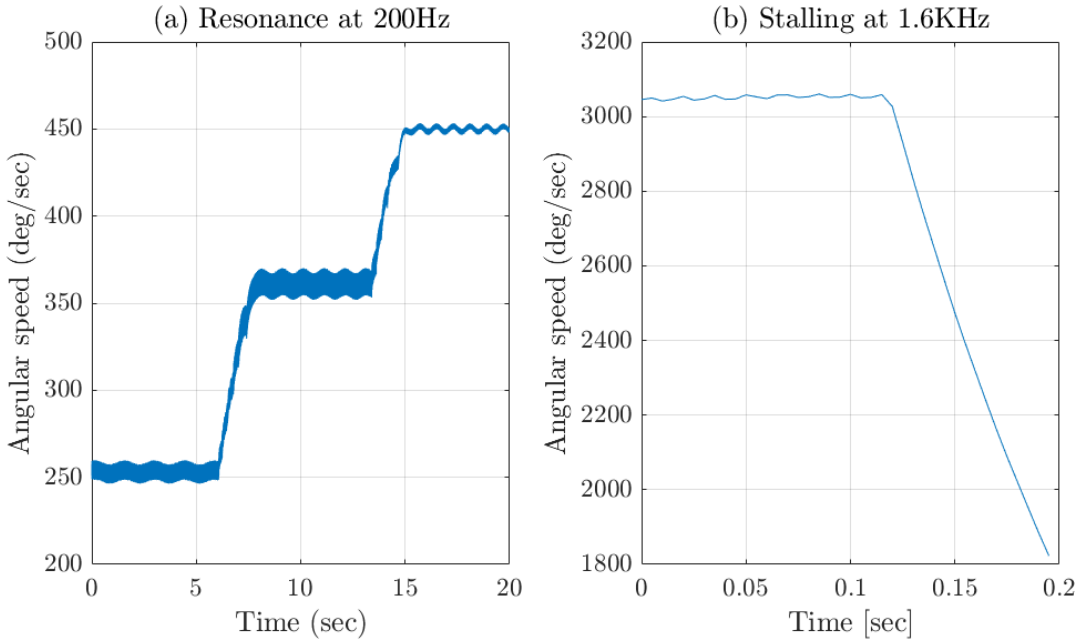

Figure 10: Motor resonance and Stalling with the load attached

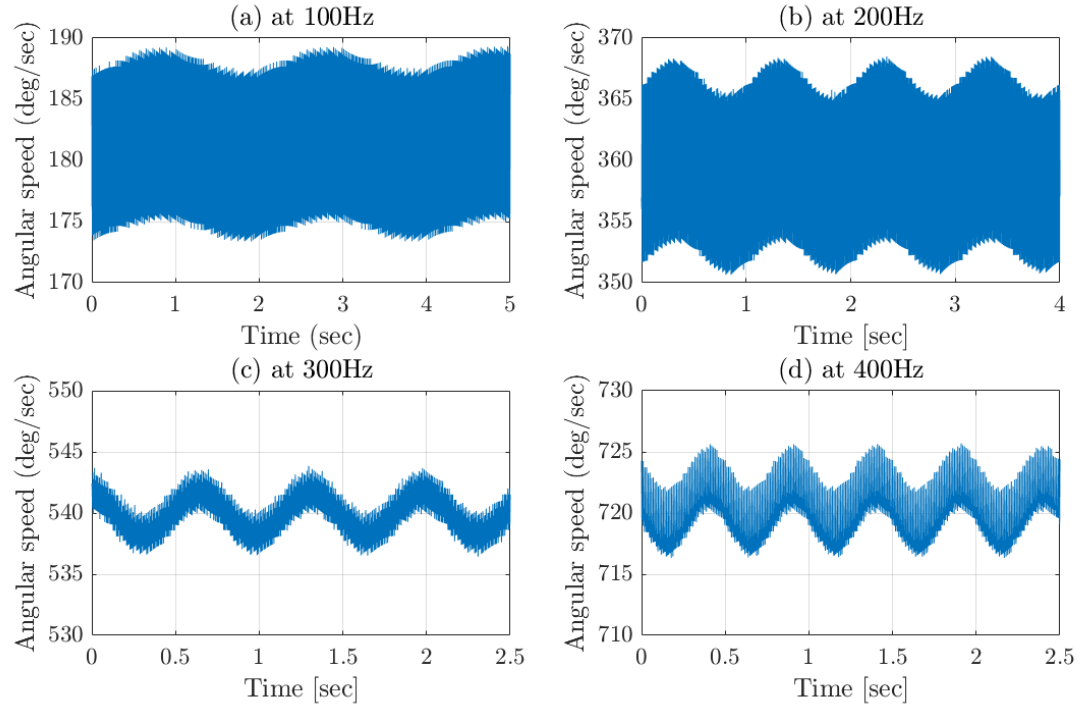

Figure 11: Motor performance at integral multiples and integral fractions of natural frequency

Without Load (10): Similar experiment is conducted for the system without the load attached to the shaft of the motor. The motor is first excited at its natural frequency which is

experimentally found out to be 210Hz as shown in figure 12(a) (where the system is excited at 210Hz and 310Hz) which differs by 3.5% from the theoretically computed natural frequency of 217Hz. Next the system is excited at integral fraction (105Hz) and integral multiple (420Hz) of the natural frequency and compared to an arbitrary frequency (300Hz) as shown in figure 13. The response at the integral fractions and the integral multiples are as expected, as having a high band of velocity with high vibrations (excitations). However, there is no unstable performance found at these step-rates. Increasing the frequency to 1.8KHz results in the system losing synchronization and resulting in the stalling of the motor as seen in figure 12(b).

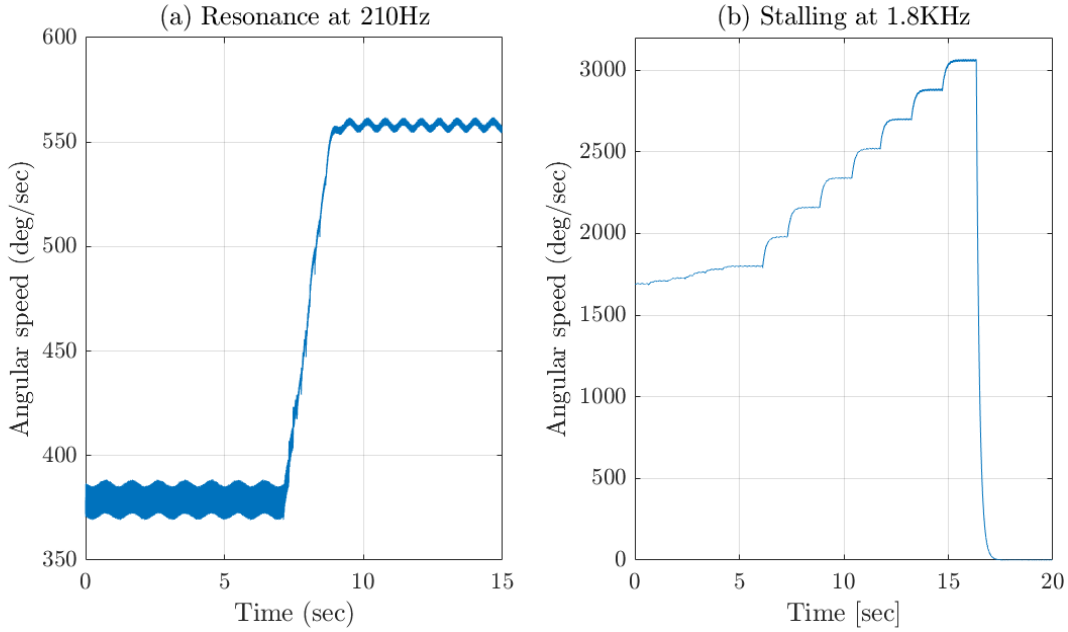

Figure 12: Motor resonance and Stalling without the load attached

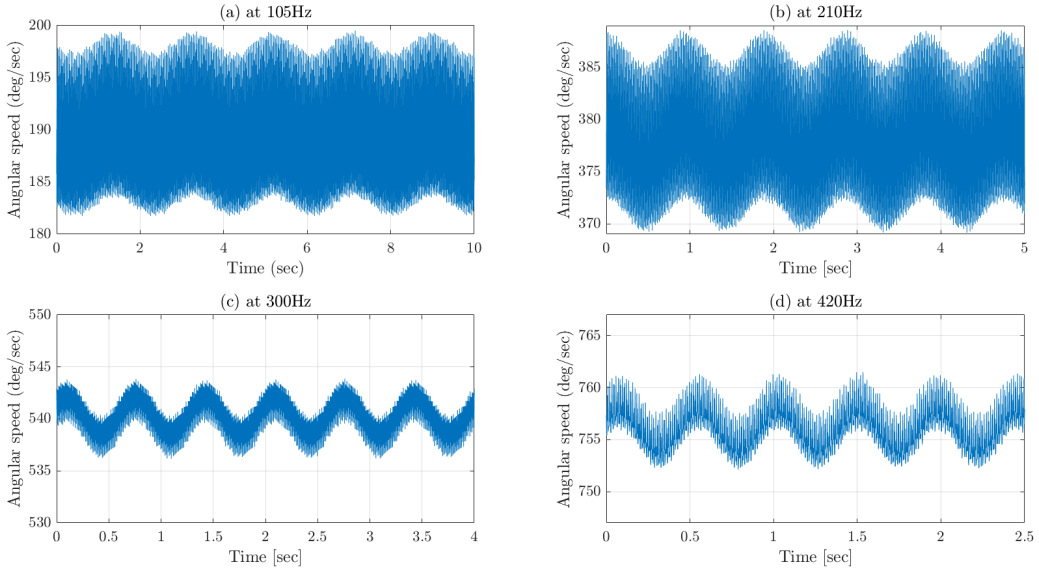

Figure 13: Motor performance at integral multiples and integral fractions of natural frequency

(b) Pull-in and Pull-out Step-Rate (22)

To determine the pull-in and pull-out characteristics (i.e. determining the maximum step-rate of the motor when increased instantly and when increased gradually respectively), a pulse train command of 'X' step-rate (frequency) is given to the motor via a function generator.

Pull-in step-rate:
Pull-in step-rate corresponds to the step-rate or the speed of the motor when the step-rate of the pulse train is instantly increased from 0 to 'X' steps per second.

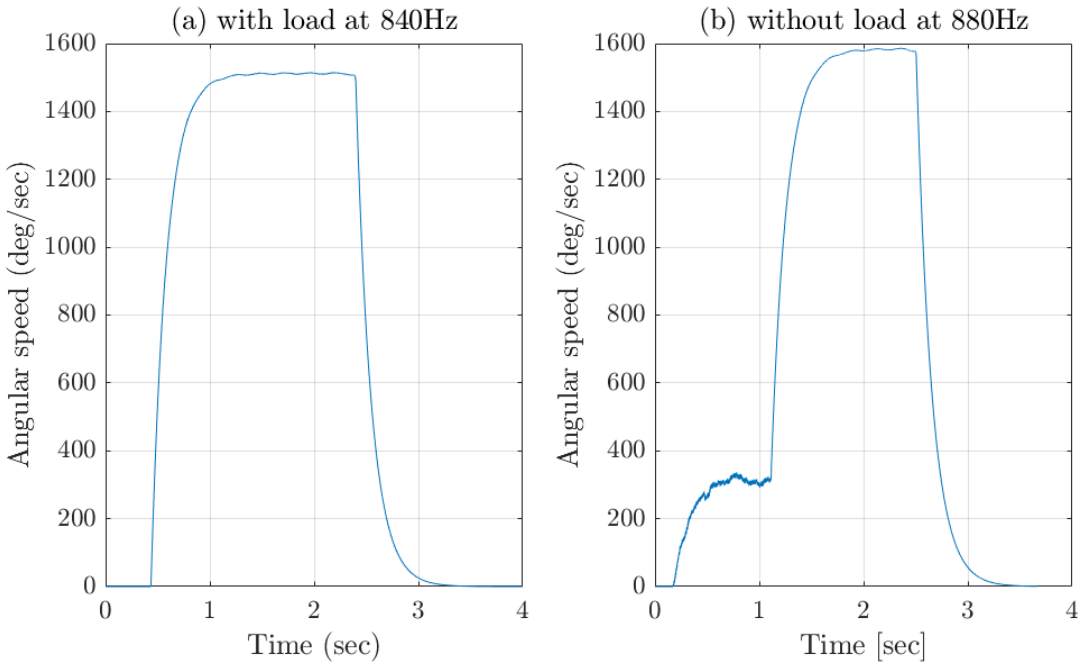

Figure 14: Pull-in step-rate characteristic

With Load (5):
The pull-in step-rate of the motor is experimentally observed to be 840Hz which corresponds to the theoretical angular speed of 1512 deg/sec. As shown in figure 14(a) the motor exhibits a maximum angular speed of 1515 deg/sec, thus producing an error of 0.2%.

Without Load (5):
The same experiment is repeated for the motor but without the load. The pull-in step-rate is observed to be 880Hz which corresponds to 1584 deg/sec. However the motor exhibits a maximum angular speed of 1586 deg/sec as shown in figure 14(b) thus producing an error of 0.14%.

Pull-out step-rate:
As mentioned briefly before, the pull-out step-rate corresponds to the step-rate or speed of the motor when the pulse train given to the motor is increased gradually from zero to 'X' steps per second. A use of function generator is specially useful for this section of experiment, as was found that the simulate signal block in the LabVIEW VI was not able to generate and compute the signals at such high frequency and the system was constantly losing synchronization.

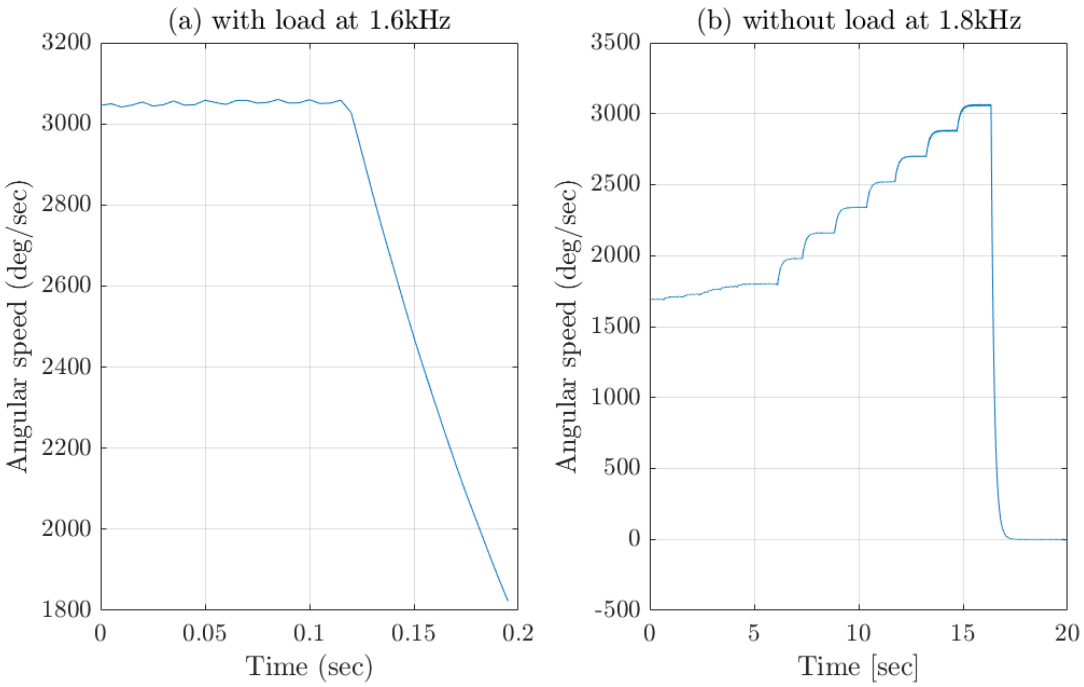

Figure 15: Pull-out step-rate characteristic

With Load (5):
Pull-out step-rate of the motor with load attached is observed to be 1.6KHz which corresponds to the theoretical value of 2880 deg/sec. The maximum angular velocity of the motor is however observed as 3060 deg/sec as can be seen in the magnified response of the motor in figure 15(a). This produces an error of 6.26% from the theoretically computed value.

Without Load (5):
The experiment is repeated for the setup without the load attached to the motor. The pull-out step-rate is measured to be 1.8KHz which corresponds to a theoretical maximum angular velocity of 3240 deg/sec. However the maximum angular velocity of the motor as seen in figure 15(b) is measured as 3069 deg/sec, thus producing an error of 5.3% from the theoretical maximum angular velocity.

The error corresponding to the theoretical maximum angular velocity and the measured angular velocity increases significantly in the case of pull-in and pull-out. This discrepancy appears in the experiment because of the lack of accuracy in the frequency generated by the function generator. The resolution of the function generator is found to be 100Hz after it crosses a frequency of 1KHz. Whereas, the motor can have a maximum angular velocity corresponding to a pull-out step-rate of 1750Hz (as is the case of without load), which the function generator is not able to generate because of its limited resolution.

Comparison of Pull-in and Pull-out Step-Rate: When the stepper motor was tested for two cases of increasing step-rate suddenly and gradually, the observed maximum step-rate of the motor differed significantly as mentioned previously for both with and without

load.

With Load (1): The stepper motor reached maximum speed of 840 Hz and 1.6kHz when the step-rate was suddenly and gradually increased, respectively. The maximum speed reached with gradual increase in step-rate is higher than that of the sudden increase because of inertia. The pull-in torque greatly depends on the inertia of the motor and load, while the pull-out torque is not dependent on the load attached to the motor. The difference in the maximum speed is due to the stepper motor requiring less torque when speed is gradually increased. When the motor is suddenly commanded a step-rate, it requires torque for accelerating and due to limited torque, the stepper motor is also limited in maximum speed. Thus, the stepper motor accomplishes higher speed with gradual increase in step-rate.

Without Load (1): The stepper motor without load reached maximum speed of 880 Hz and 1.8kHz when the step-rate was suddenly and gradually raised, respectively. Not only is there a difference in the maximum speed depending on step-rate, but also the difference between the maximum speed to that of the stepper motor with load is substantial. The stepper motor has different maximum speed depending on the step-rate increase due to the impact of inertia and the necessary torque required to accelerate suddenly from 0 to commanded step-rate. Also, the maximum speed of the motor without load is higher than that of the motor with load because decrease in load reduces the torque required to rotate the shaft and achieve its commanded speed.

4 Motion Control (25pts)

The motion control of the stepper motor with load attached is created for a trapezoidal velocity profile in figure 16. The constraints of this profile are:

1. The total motion (i.e. area under the velocity curve) should be 1440 deg($\pm$ 10deg)
2. The region of constant speed should be at least 1080 deg (or 3 full rotations)
3. The constant speed should be 180 deg/sec
4. The fluctuations/oscillations of speed in the constant speed region should be <5% of the constant speed value

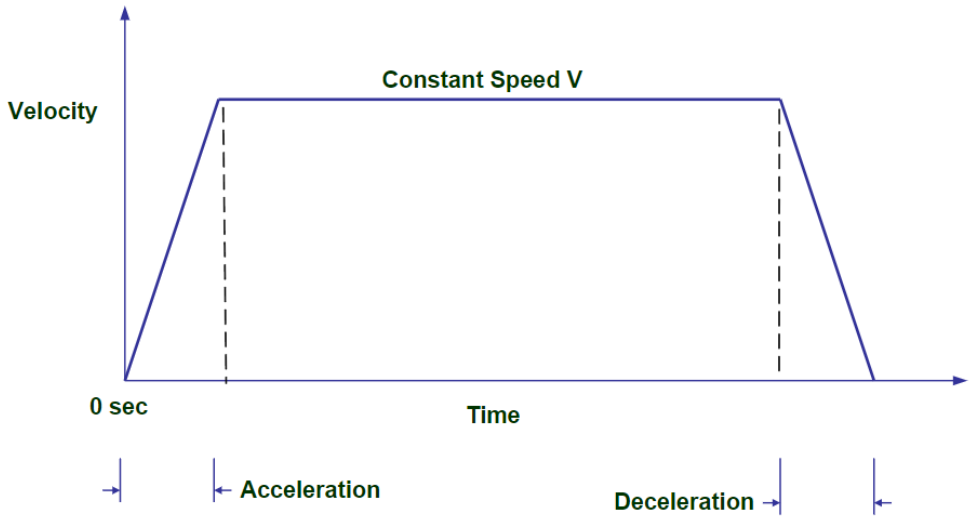

Figure 16: Trapezoidal velocity profile required for motion control.

(a) Full, Half, and Quarter Stepping Modes (15)

The stepper motor was commanded to create the trapezoidal velocity profile shown in figure 16 for different stepping modes. However, the motion criteria was not achievable for quarter stepping due to the limitation of the LabVIEW computation time. A velocity of 180 deg/sec for quarter stepping requires a pulse-train command frequency of 400Hz. For the LabVIEW to command such a high frequency without finishing late on its computation, the required loop time must be at least 0.00125 seconds due to impact of Nyquist frequency. Despite reducing the computation required in the LabVIEW, the computation time was not able to be reduced to 0.00125 seconds per loop. Thus, quarter stepping was not achieved for motion control. On the other hand, motion control with full and half stepping was achieved and is shown in figure 17.

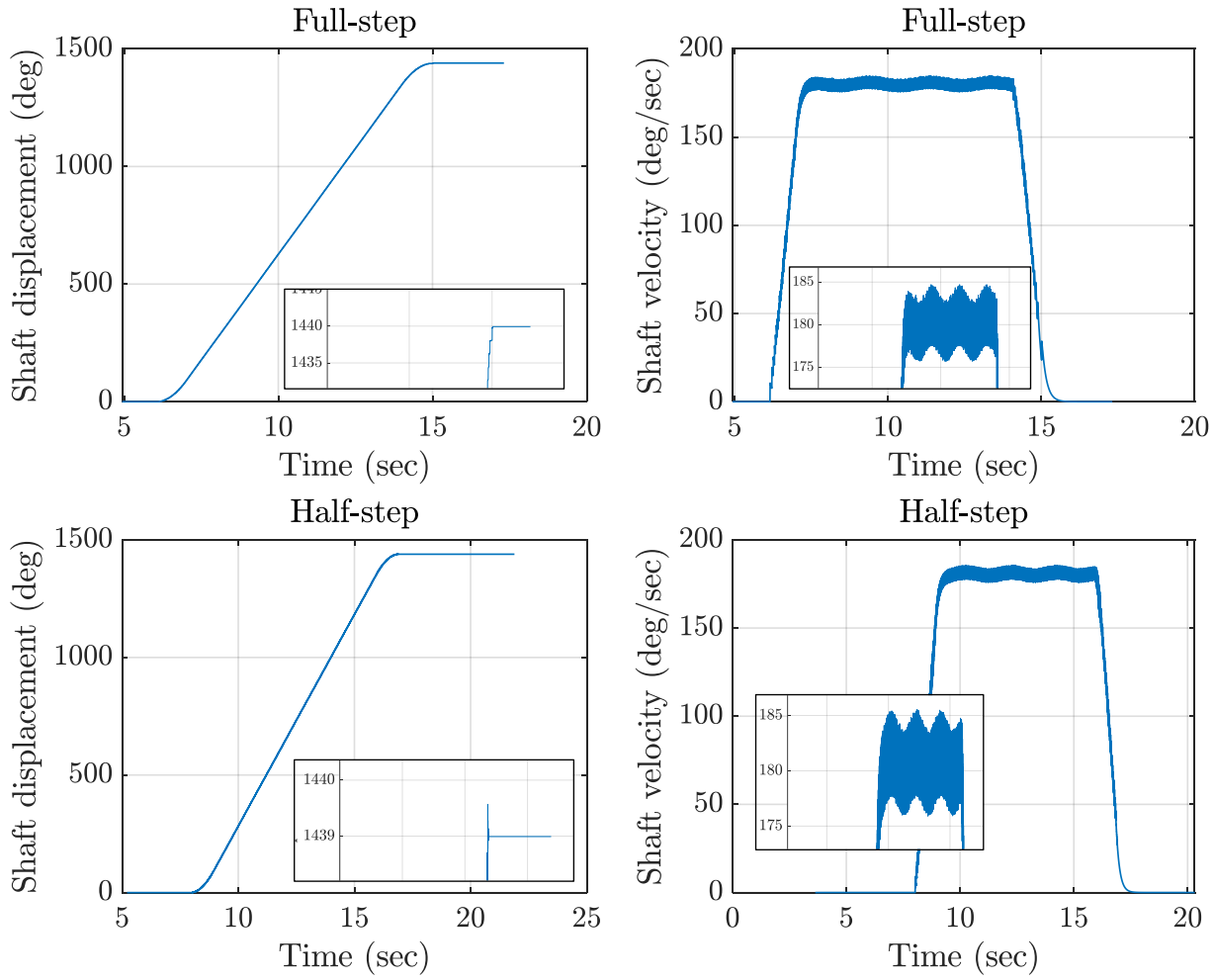

Figure 17: Velocity Control of stepper motor in full-step at half-step modes. The zoomed in portions of the graphs are shown to indicate that the constraints are fulfilled.

Figure 17 shows the stepper motor shaft responding to the motion control command for full-step and half-step modes. A total shaft angular displacement of 1440 and 1439 degrees respectively is obtained and fits constraint 1, the requirement of total motion of 1440 $\pm$ 10 degrees. For the constant speed region, shaft speeds for the respective modes vary within [177,185] deg/s and [176,185] deg/sec, resulting in a fluctuation of $\sim$ 2.5% about the desired constant speed of 180 deg/s, fulfilling constraint 3 and 4 with constant speed of 180 deg/s and fluctuations $<$ 5%. During this period, shaft angles traversed are 1220 deg and 1222 deg for full and half-step, respectively, fulfilling constraint 2 constant speed displacement region $>$ 1080 deg . As mentioned previously, we were unable to perform quarter stepping as the LabVIEW simulation loop would always finish late and the stepper motor would eventually stall. Figure 18 and figure 19 shown below give the LabVIEW block diagram and LabVIEW front panel drawn for motion control of the stepper motor shaft.

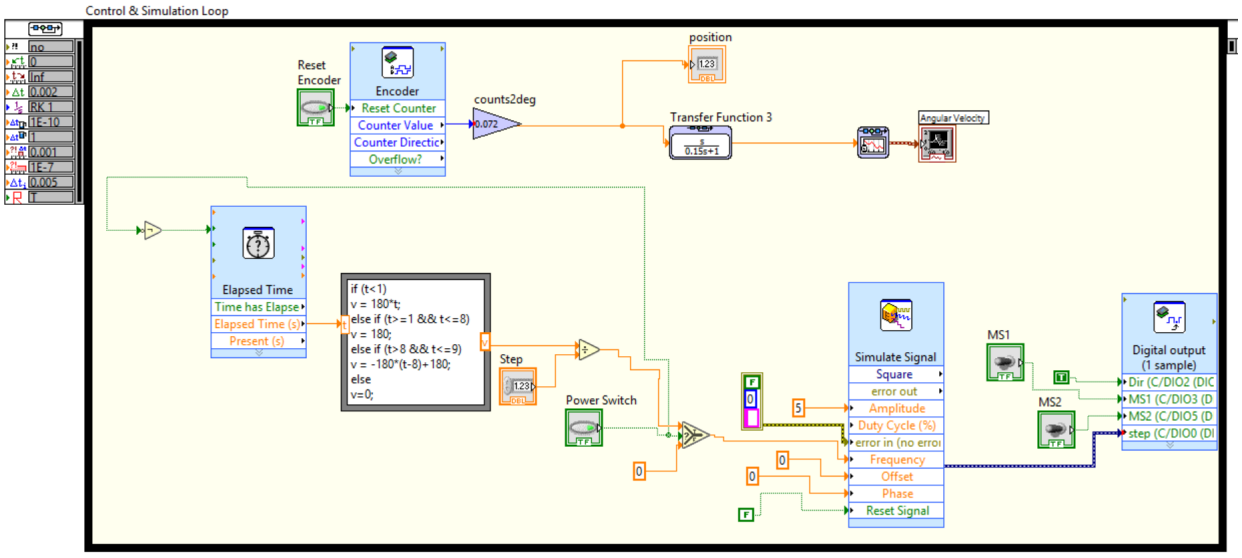

Figure 18: LabVIEW block diagram for motion control. The LabVIEW VI was simplified to further reduce the computational load on myRio.

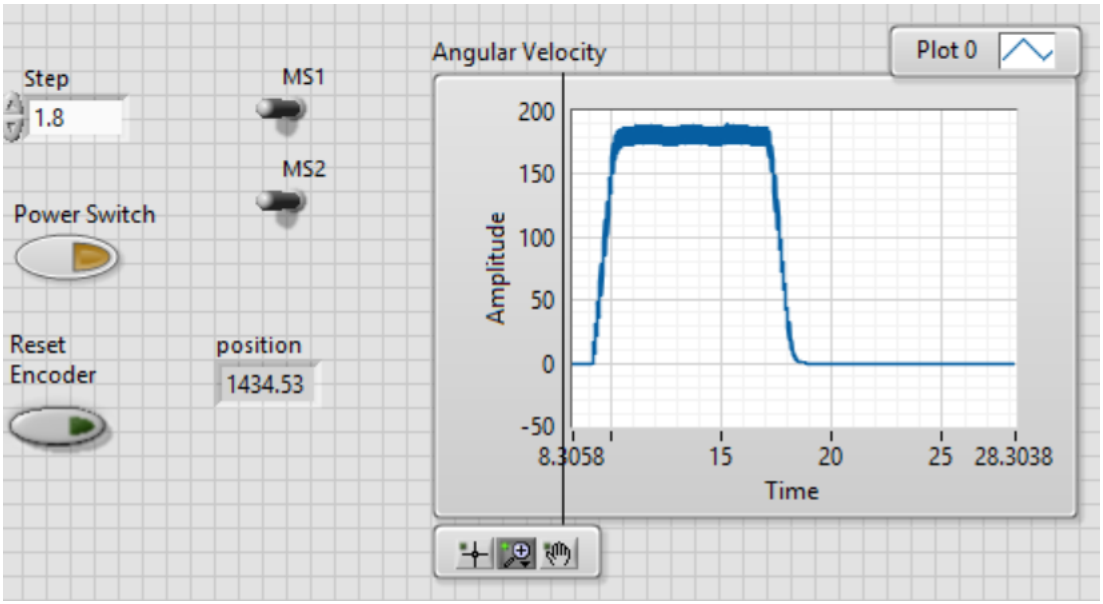

Figure 19: LabVIEW front panel for motion control in full-step mode. MS1 and MS2 have both been set to low. An area under the velocity curve of 1434.53 degrees is obtained, well within the requirements of 1440 ± 10 degrees.

(b) Motion Performance for Various Stepping Modes (5)

With the current VI, the stepper motor was able to fulfill all design constraints for motion control in the full-step and half-step modes. Figure 20 compares stepper motor performance in full-step and half-step modes. Firstly, since at half-step we have a sampling frequency for

myRio (500 Hz) more than twice that of the pulse train (200 Hz), we are able to capture the approximately second order behavior of the rotor shaft shown by the decaying oscillations per step, as can be seen in the graphs on the left and in the center. At full step, the myRio sampling frequency (200 Hz) is exactly twice that of the pulse train (100 Hz). This may be causing aliasing, leading to step like readings as observed. We must remember that the encoder has a resolution of 0.072 deg, hence for the given stepping rates, a sufficiently high sampling frequency can give us an analog like reading. Secondly, the pulse trains corresponding to full-step and half-step are at 100 Hz and 200 Hz respectively. As already reported in previous sections, the natural frequency for the stepper motor with load on is $\sim$ 200 Hz. Hence, it is not surprising that we see resonance being triggered when the stepper motor operates at 180 deg/sec, as recorded in the graph on the right. Thirdly, in both modes, no steps were skipped as the area under the Velocity vs. Time curve was 1440 deg and 1439 deg respectively.

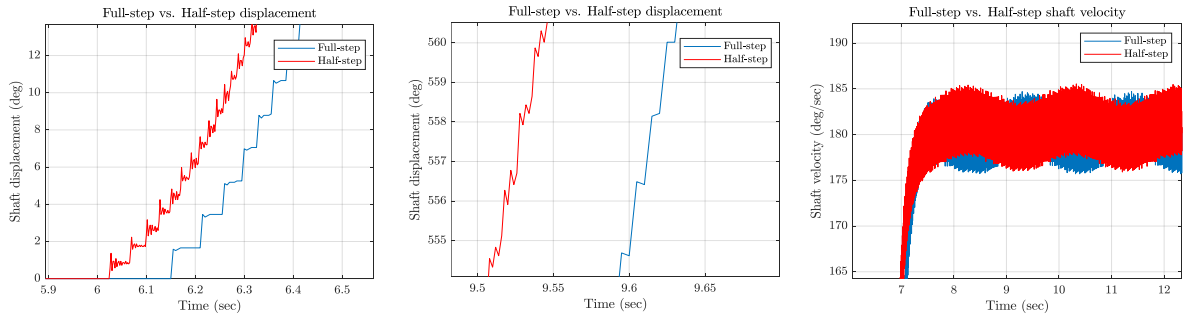

Figure 20: Comparing stepper motor performance for Full-step and Half-step modes. Graphs on the left and in the center compare shaft displacements while the graph on the right compares shaft velocities.

We were able to achieve required stepper motor performance in full-step mode (step frequency = 100 Hz) with the VI from Q2 (loop time = 5 msec). However, initially for half stepping, due to an increased step frequency (= 200 Hz) and a required reduced loop time (= 2 msec), the VI computation was unable to keep pace with the looping of the LabVIEW blocks, resulting in it losing synchronization. This would often result in the stepper motor shaft skipping steps and traversing a shaft angle much lesser than 1440 deg. Clearing blocks that were unnecessary for motion control yielded the diagram shown in figure 18. This VI was able to perform half stepping. However, we were never able to conduct quarter stepping since the VI continued to lose synchronization.

(c) Maximum constant speed of the set-up (5)

As already explained earlier, the current LabVIEW implementation allowed no more than half-stepping. The maximum loop rate that the LabVIEW can compute without finishing late was 0.002 seconds, resulting in maximum myRio sampling frequency to be 500 Hz. Thus, the maximum pulse-train command frequency without causing aliasing was expected to be 250 Hz, the Nyquist frequency. To maximize constant speed, we chose to drive the

stepper motor at full-step, sending pulse trains at 250 Hz. This corresponds to a maximum stepper motor constant speed of 450 deg/sec. As can be seen in Figure 21, we did reach this maximum permissible speed. Attempting to drive the motor at higher speeds by sending higher frequency pulse trains would cause it to stall due to aliasing. Attempting to increase sampling frequency of myRio to 1000Hz would cause the LabVIEW implementation to lose synchronization, resulting in the motor rotor skipping steps. If we were to use half-step, the maximum speed would be 125 Hz. Hence, our implementation was limited to driving the stepper motor driver at a constant speed of no more than 450 deg/sec with full-step.

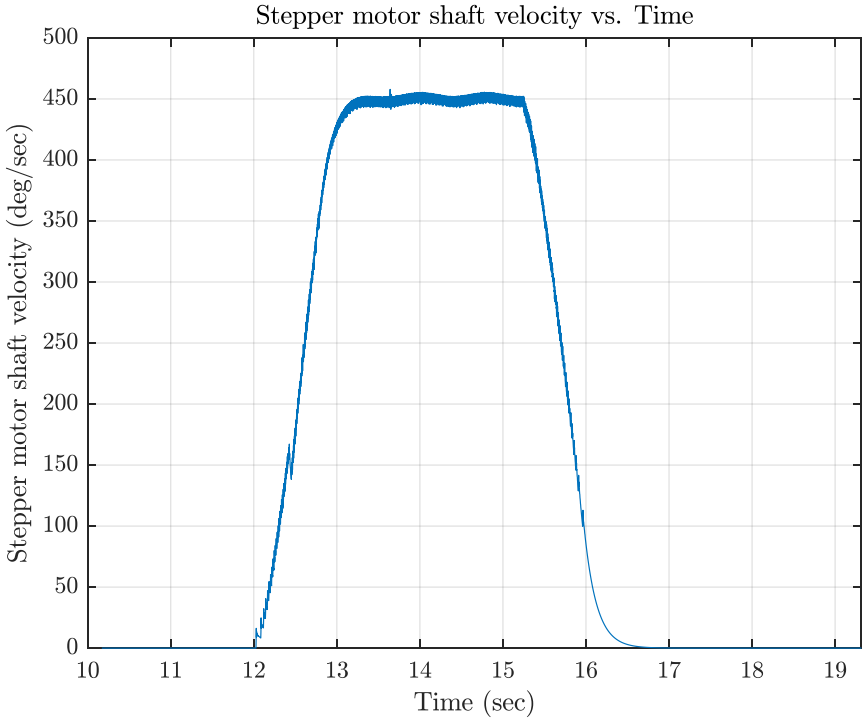

Figure 21: Maximum constant speed of the set-up.